Published in final edited form as:
Nat Cell Biol. 2013 November ; 15(11): . doi:10.1038/ncb2856.

Cytonemes are required for the establishment of a normal Hedgehog morphogen gradient in *Drosophila* epithelia

Marcus Bischoff[#2,3,4], **Ana-Citlali Gradilla**[#1], **Irene Seijo**[1], **Germán Andrés**[1], **Carmen Rodríguez-Navas**[1], **Laura González-Méndez**[1], and **Isabel Guerrero**[1,4]

[1]Centro de Biología Molecular "Severo Ochoa" (CSIC-UAM), Nicolas Cabrera 1, Universidad Autónoma de Madrid, Cantoblanco, E-28049 Madrid, Spain.

[2]Department of Zoology, University of Cambridge, Downing Street, Cambridge, CB2 3EJ, UK

[#] These authors contributed equally to this work.

Summary

Hedgehog (Hh) signalling is important in development, stem cell biology and disease. In a variety of tissues, Hh acts as a morphogen to regulate growth and cell fate specification. Several hypotheses have been proposed to explain morphogen movement, one of which is transport via filopodia-like protrusions called cytonemes. Here, we analyse the mechanism underlying Hh movement in the wing disc and the abdominal epidermis of *Drosophila*. We show that, in both epithelia, cells generate cytonemes in regions of Hh signalling. These protrusions are actin-based and span several cell diameters. Various Hh signalling components localise to cytonemes, as well as to punctate structures that move along cytonemes and are probably exovesicles. Using *in vivo* imaging, we show that cytonemes are dynamic structures and that Hh gradient establishment correlates with cytoneme formation in space and time. Indeed, mutant conditions that affect cytoneme formation reduce both cytoneme length and Hh gradient length. Our results suggest that cytoneme-mediated Hh transport is the mechanistic basis for Hh gradient formation.

INTRODUCTION

Morphogen signalling is crucial for developmental patterning. Morphogens are secreted molecules that act at a distance and in a concentration-dependent manner, controlling the differential activation of target genes according to the distance from their source[1]. To generate this activity gradient, morphogen production, transport and reception must be tightly controlled.

The mechanism of morphogen movement from producing to receiving cells has been the subject of intense study[2]. Several models have been proposed, including restricted diffusion[3], planar transcytosis[4], movement by exosomes[5] or argosomes[6] and lipoprotein particles[7], and transport by cellular extensions called cytonemes that orient towards the morphogen source. Cytonemes were first identified in the *Drosophila* wing disc, where they

[4]Corresponding authors: Iguerrero@cbm.uam.es Phone: Office: +34 91 196 4680. Lab: +34 91 196 4465. mb273@st-andrews.ac.uk Phone: +44 1334 467199. .

AUTHOR CONTRIBUTIONS: MB designed and performed experiments, analysed data and wrote the paper; ACG performed experiments and analysed data; IS and LGM performed experiments; GA designed and performed experiments and analysed data; CRN generated constructs for Flo2 overexpression and helped with RNAi screening and generating mutant clones; IG designed and performed experiments, analysed data and wrote the paper.

[3]Current address: Biomedical Sciences Research Complex, University of St Andrews, North Haugh, St Andrews, KY16 9ST, UK

COMPETING FINANCIAL INTERESTS: The authors declare no competing financial interests.

Europe PMC Funders Author Manuscripts

have been postulated to connect sending and receiving cells, enabling transfer of surface-associated cargoes[8,9]. However, the involvement of cytonemes in morphogen transport is still mysterious and the mechanisms underlying cytoneme function are still elusive.

To study the role of cytonemes in morphogen gradient formation, we investigated Hh signalling in two experimental paradigms in *Drosophila*, the wing disc and the abdominal epidermis. Hh acts as a morphogen, specifying cell identities in initially homogenous fields of cells[2,10]. Hh is post-translationally modified by the addition of cholesterol[11] and palmitic acid[12], which confer a highly hydrophobic character on Hh. These modifications suggest that association with cell membranes or lipoprotein particles is involved in Hh transport[11].

In the wing disc, Hh patterns the central region of the wing[13,14]. The wing is divided into anterior (A) and posterior (P) compartment[15]. P compartment cells produce Hh, which moves across the compartment border, decreasing in concentration as it spreads into the A compartment[16,17]. Dependent on this signal, the Hh receptor Patched (Ptc) is upregulated in a graded manner in the A compartment[18,19]. Ptc can thus serve as readout of Hh signalling.

In the abdominal epidermis, Hh also acts as a morphogen and is expressed in the P compartment[20,21]. Since the abdomen comprises multiple segments, Hh influences A compartment cells both anteriorly and posteriorly of its source[20]. In the larval epithelial cells (LECs), Ptc is expressed in A compartment cells anterior and posterior to each P compartment[20]. In the adult histoblasts, Ptc is expressed in a graded manner anterior to and in a narrow stripe posterior to each P compartment[20-22]. This pattern of Ptc expression is established during adult tissue formation. Ptc expression starts in the anterior dorsal histoblast (ADH) nest[23] before it fuses with the posterior dorsal histoblast (PDH) nest at the beginning of the process[21] (initially, both nests are separated by a row of LECs[23]). Histoblasts then spread and replace the LECs[23]. Only after histoblasts have met at the segment (P/A) border, Ptc expression begins in the histoblast stripe posterior to the P compartment[22].

To understand how Hh is released and transported, analysis of the Hh co-receptor Interference hedgehog (Ihog)[24] has proven useful. *Drosophila* Ihog interacts directly with the glypican Dally-like (Dlp), Hh and Ptc in the A compartment[25-27]. It is necessary for membrane localisation of Ptc[24] and required to maintain normal extracellular Hh levels[26,28]. We have recently described that fluorescently tagged forms of Ihog localise to the plasma membrane and label cellular processes in the baso-lateral part of wing discs[28]. We refer to these processes as ‘cytonemes’, as they resemble the previously described processes implicated in morphogen transport[8].

Here, we characterise these cytonemes in detail and study their role in Hh gradient formation. We show that, in the wing disc and in the abdominal epidermis, cytonemes are present in the Hh morphogenetic field. Hh and several Hh signalling components localise to these actin-based protrusions. Interestingly, we observe punctate structures, probably exovesicles, some of which are associated with and move along cytonemes. Using *in vivo* imaging, we show that cytonemes extend and retract dynamically and that Hh gradient establishment correlates with cytoneme formation in space and time. Furthermore, we found a strong correlation between maximum cytoneme length and Hh gradient length. These results strongly suggest that cytonemes play a role in Hh gradient establishment. Overall, our data support a model of Hh transport in which cytonemes act as routes for Hh movement in the extracellular matrix (ECM).

RESULTS

Wing disc cells generate basal actin-based cytonemes

To analyse wing disc cytonemes[28] in detail, we expressed fluorescently tagged Ihog in either A or P compartment cells. We found that both cell types displayed these processes basally (Fig. 1a-e). P compartment cells extended a dense array of shorter cytonemes (~27 μm long) and individual longer cytonemes (up to 70 μm long) perpendicular to the A/P border into the neighbouring compartment. Cytonemes of A compartment cells were about 40-50% shorter than P compartment cytonemes. The processes were mostly linear (0.1-0.2 μm diameter), but some were branched, especially towards their distal end. The cytonemes covered most of the Hh gradient in the A compartment (7-12 cell diameters). We could also detect lateral processes, but these were considerably shorter (1-2 cell diameters).

Fluorescently tagged Ihog also labelled punctate structures, some of which decorated cytonemes (Fig. 1f). Other puncta were not associated with cytonemes and were located laterally in a region apical to the basal cytonemes (Fig. 1f). To explore whether these puncta could be exovesicles, we performed immunoelectron microscopy of wing discs expressing Ihog-CFP in P compartment cells. Immunogold labelling with α-GFP antibodies detected Ihog at baso-lateral plasma membranes of P compartment cells (Fig. 1g,h), including cytoplasmic protrusions (Fig. 1g), and in clusters of exovesicles (50 to 200 nm) present in discrete baso-lateral extracellular spaces (Fig. 1h).

Besides fluorescently labelled Ihog, cytoskeletal markers such as Moe-Cherry (Fig. 2a) and GMA (an actin-binding fragment of Moesin that labels actin filaments[29]; Fig. 2b) labelled cytonemes. This corroborates the notion that cytonemes are actin-based structures as previously reported[8]. Moreover, various membrane markers labelled cytonemes. Fluorescently labelled Flotillin-2 (Flo2/Reggie-1), a major component of membrane microdomains[30], as well as CD4-Tomato[31] and glycosylphosphatidyl-inositol-YFP (GPI-YFP)[6] localised to cytonemes (Fig. 2c,d,e). Similar to Ihog, these markers also labelled puncta along cytonemes (Fig. 2d,e).

Interestingly, cytonemes were more easily visible when Ihog was co-expressed (Fig. 2e-g) than when cytoskeletal and membrane markers were expressed alone (Fig. 2a-d). It is hence possible that Ihog stabilises cytonemes, maybe by recruiting some actin-stabilising factor. That cytonemes could be observed without Ihog overexpression using a variety of markers showed that cytonemes were not an Ihog overexpression artefact.

Hh pathway components label cytonemes

If cytonemes were involved in morphogen signalling, they would be expected to carry signalling pathway components[9]. Indeed, we have previously observed that Ihog overexpression increases Hh levels along cytonemes[28,32]. We thus examined whether we could detect Hh pathway components other than Ihog along cytonemes. Using α-Hh antibody or Hh-GFP, we found Hh in puncta that appeared to be organised in threads running perpendicular to the A/P border in the basal part of the wing disc epithelium (Fig. 3a,b). These structures became more evident after we 'froze endocytosis' by expressing a dominant negative form of Dynamin (Shi^{K44A}) or by using a temperature-sensitive *dynamin* mutant (shi^{ts1}) before staining for Hh or Ptc (Fig. 3c-e). Freezing endocytosis leads to an accumulation of Hh or Ptc prior to internalisation, which improves their visualisation[33].

In addition, Dispatched (Disp), which is required for Hh release[34], and Dlp, which is required for both Hh release[28] and reception[35], localised to basal protrusions (Fig. 3f,g). These findings confirm that Hh pathway components are associated with cytonemes.

Cytonemes are present at sites of Hh signalling in the abdominal epidermis

To study cytonemes *in vivo*, we turned to the abdominal epidermis for live imaging. Using fluorescently labelled Ihog and a GFP-trap in the *ptc*-promotor (*ptc-promotor-trap::GFP*) allowed us to label cytonemes and simultaneously monitor Ptc expression (Fig. 4a; Supplementary Fig. S1a). We found that both histoblasts and LECs of P compartment cells generated basal cytonemes, resembling the protrusions in wing discs (Fig. 4b-f). Importantly, the presence and length of these protrusions spatially correlated with Ptc expression, both at the compartment (A/P) and segment (P/A) borders in larval and adult epithelia (Supplementary Fig. S1b):

Histoblasts—(1) *At the compartment border:* P compartment histoblasts generated protrusions that reached anteriorly into the A compartment, covering most of the Ptc-promotor-trap::GFP gradient (Fig. 4b,c; Supplementary Videos S1,S2). We observed both a dense array of shorter protrusions (about 17 μm, 4 cell diameters) and individual longer protrusions (about 40 μm, ~9 cell diameters). These protrusions could also be observed by labelling the actin cytoskeleton with Utrophin-GFP[36] (Supplementary Fig. S1c,d). In contrast to P compartment histoblasts, A compartment histoblasts rarely sent shorter cytonemes posteriorly into the P compartment (Fig. 4d; Supplementary Video S3). This is a prominent difference to wing discs, where both A and P compartment cells produced cytonemes extensively (Fig. 1b,d). (2) *At the segment border:* P compartment histoblasts very rarely sent short protrusions posteriorly into the neighbouring segment (Fig. 4b). This correlated with the short-range signalling event occurring at this boundary – here, only a narrow stripe of histoblasts switched on *ptc* expression[22].

LECs—(1) *At the compartment border:* P compartment LECs sent protrusions anteriorly into the A compartment (Fig. 4e; Supplementary Video S4), where also Ptc expression could be observed (Fig. 4a). (2) *At the segment border:* P compartment LECs sent thick bundles of cytonemes posteriorly, which ‘surrounded’ the first row of A compartment LECs of the neighbouring segment (Fig. 4f; Supplementary Video S5). This row of cells also expressed Ptc-promotor-trap::GFP (Fig. 4a).

Our observation of threads of Hh puncta running perpendicular to the compartment border (Fig. 3a,b) suggested that cytonemes might be oriented along the anterior-posterior (a-p) axis. To test this hypothesis, we generated FLP-out clones in abdomen, which expressed Ihog-RFP. These clones confirmed that P compartment cytonemes point anteriorly (Supplementary Fig. S1e,f).

Cytoneme formation and Hh signalling gradient establishment correlate over time

Using live imaging also allowed us to explore how Hh signalling and cytonemes behave over time. Before histoblast nest fusion, Ptc-promotor-trap::GFP expression could be observed in the ADH nest. Only after ADH and PDH nests had fused, histoblast cytonemes started to form (Fig. 5a-c; Supplementary Videos S2, S6). Simultaneously, Ptc expression in the ADH nest began to increase (Supplementary Video S6). Early Ptc-promotor-trap::GFP expression therefore seems to be independent of cytonemes. Eventually, the cytonemes grew and the Ptc gradient formed (Supplementary Videos S2,S6). Intriguingly, maximum cytoneme length correlated with Hh activity gradient length throughout development (Fig. 5d-f; Supplementary Video S6). Furthermore, the shape of the Hh activity gradient and the density of cytonemes along the a-p axis correlated: The short array coincided with the brightest section of the gradient; then both curves declined similarly (Fig. 5d; Supplementary Video S7). This correlation was also observed in wing discs (Supplementary Fig. S2).

Also the formation of the thick cytoneme bundles of P compartment LECs (Fig. 4f) correlated with the onset of Ptc expression in the receiving cells (Supplementary Video S2). Overall, our findings show that cytonemes and Hh signalling are closely associated in space and time.

Cytonemes are dynamic structures

Next we analysed the behaviour of individual cytonemes. As in wing discs, Ihog-RFP/-CFP expression stabilised cytonemes also in abdomen – we could observe individual protrusions for up to 9.5 hours. To study cytoneme dynamics, we therefore used GMA instead of Ihog-RFP/CFP to visualise cytonemes. Without Ihog, histoblast cytonemes appeared thinner and shorter (up to 26 μm) (Fig. 5g,h; Supplementary Video S8) and had a lifetime of about 11 ± 2.6 min (n=6) (Supplementary Video S9). With a growth rate of approx. 5 μm/min, they grew faster than filopodia observed in other *in vivo* systems (3.3 μm/min[37]) and *in vitro* assays (2.5 μm/min[38]). Cytonemes were very dynamic; they grew to their final length and immediately shrank (Supplementary Fig. S3; Supplementary Video S10). We could also image cytonemes using the membrane markers CD4-Tomato[31] and Gap43-Venus[39] (Supplementary Videos S11,S12).

Interfering with cytoneme formation affects the Hh gradient

Our observations suggest that cytonemes might be important in Hh transport. Thus, a manipulation of cytoneme formation should affect the Hh gradient. To test this hypothesis, we manipulated cytonemes in wing discs using RNAi against various actin-binding proteins and analysed the effects on gradient formation. We chose the following proteins: **(1) Capping protein (CP):** CP restricts the accessibility of actin filaments, thus inhibiting addition or loss of actin monomers[40]. In *Drosophila*, mutations in either subunit (*cpa* or *cpb*) lead to accumulation of F-actin[41]. In accordance with this, we found an accumulation of actin and myosin in wing disc cells after Cpa-RNAi (Supplementary Fig. S4). Cell culture experiments with a CP inhibitor have furthermore shown that at high inhibitor concentrations, actin polymerisation is inhibited[42]. **(2) SCAR:** SCAR/WAVE is involved in the generation of lamellipodia[43] and filopodia[44,45]. Loss of SCAR function results in the loss of F-actin and protrusions within the baso-lateral domain of the *Drosophila* pupal notum without affecting cell morphology, size, polarity or endocytosis[46]. **(3) Pico:** Pico/Lamellipodin interacts with Ena/Vasp actin regulators and is involved in lamellipodia formation[47]. We found that RNAi knock-down of all these proteins in the P compartment affected maximum cytoneme length as well as Hh gradient length, both of which were significantly shorter compared to wild-type (Figs. 6a-d,g-j; 7a,b).

In contrast, ectopic expression of Flo2/Reggie-1 in the P compartment extended the Hh gradient. Also cytonemes were longer compared to control experiments (Figs. 6e,k; 7a,b). This agrees with the observation that overexpression of Flo2/Reggie-1 induces filopodia-like protrusions in various cell lines[48]. It furthermore suggests that the mechanism by which Flo2/Reggie-1 stimulates Hh secretion and promotes its diffusion[49] might be cytoneme-related. Accordingly, knock-down of Flo2/Reggie-1 in P compartment cells produced the opposite phenotype; both cytonemes and the Hh gradient were significantly shorter than in wild-type (Figs. 6f,l; 7a,b).

Importantly, although the strength of the phenotypes varied from individual to individual, there was a strong positive correlation between cytoneme reach and gradient length for all individuals across all experiments (Fig. 7c). This strongly suggests that cytonemes play a role in Hh gradient establishment.

All above experiments were done with and without co-expression of fluorescently labelled Ihog. A comparison of gradients with and without Ihog-RFP/CFP showed that Ihog led to a shortening of the Ptc-promotor-trap::GFP gradient in both wing discs (Fig. 7d; Supplementary Fig. S5a-f) and abdomen (Supplementary Fig. S5g). This could be due to the above-mentioned cytoneme-stabilising effect of Ihog, which might impair cytoneme function. Alternatively, Ihog's ability to sequester Hh[26,28] might reduce the amount of Hh being released from cytonemes overexpressing Ihog and therefore impair signalling[32]. Our findings, however, do not represent an artefact of Ihog-RFP overexpression, because also without Ihog, the differences in gradient length between the above experiments remained (Fig. 7d). This suggests that overexpression of Ihog only affects the range of Hh signalling, but not Hh signalling *per se*.

To further rule out that our findings represent an artefact of Ihog overexpression, we replaced Ihog-RFP with the membrane marker CD4-Tomato to label cytonemes (Fig. 7e). As with Ihog-RFP, the reach of CD4-Tomato-labelled cytonemes correlated with the length of the Hh activity gradient (Fig. 7f; Supplementary Video S13). The shape of the Hh activity gradient and the density of cytonemes along the a-p axis also correlated (Fig. 7g).

In all experiments, Hh levels were not altered by the RNAi knock-down (Supplementary Fig. S6), excluding the possibility that the effects on gradient length were due to reduced morphogen levels in the signal-producing cells.

In addition, RNAi against genes involved in exovesicle production/release had a significant effect on the length of the Hh activity gradient. A range of RNAi treatments were used, including the ESCRT complex members TSG101, Alix, HRS and VPS4[50,51] as well as proteins found in exosomes, such as AnxB11 and Rab11[50]. In all experiments, a shortening of the Hh gradient was observed (Supplementary Fig. S7).

Cytoneme-mediated Hh transport

To further explore the role of cytonemes in Hh transport, we analysed the relationship of cytonemes and ECM components, such as heparan sulfate proteoglycans (HSPGs), which are known to mediate Hh transport. Toutvelu (Ttv) and Brother of ttv (Botv) are essential for the biosynthesis of HSPGs[52,53]. Hh cannot cross $ttv^{-/-}$ or $ttv^{-/-}$, $botv^{-/-}$ mutant clones abutting the A/P compartment border and can therefore not signal anterior to the clone[52,53]. However, if cytonemes were involved in Hh transport, they would be able to deliver the signal across the clone. Thus, the *ttv* mutant phenotype and the cytoneme model were only compatible, if cytonemes could not cross mutant territory. We tested this hypothesis by generating $ttv^{-/-}$, $botv^{-/-}$ mutant clones abutting the compartment border and labelling cytonemes with Ihog-YFP (Fig. 8a). We found that, in most cases, cytonemes did not cross mutant clones (Fig. 8b). As shown before[52,53], no Hh response could be detected anterior to these clones. However, if the clones were very narrow, cytonemes crossed the mutant territory (Fig. 8c) and, interestingly, we could detect a Hh response in the wild-type territory, into which the cytonemes reached.

In addition, we observed that Ihog-labelled baso-lateral puncta were only present in regions where cytonemes were present as well, but not in or anterior to mutant clones (Fig. 8b,c). This suggests that vesicles might reach their target territory via cytonemes.

These results suggest that the inability of cytonemes to cross $ttv^{-/-}$, $botv^{-/-}$ mutant clones could explain why Hh fails to signal anterior to these clones. The inability of cytonemes to cross wider clones could be due to a destabilisation of the ECM due to the lack of HSPGs, which might deprive cytonemes of structural support. Narrow clones can be crossed by cytonemes, suggesting that clones do not repel but rather destabilise them. These results not

only give a possible mechanistic explanation for the behaviour of *ttv*$^{-/-}$, *botv*$^{-/-}$ mutant clones, but also implicate cytonemes in Hh transport.

DISCUSSION

The localisation of several Hh signalling components at cytonemes[28,32] (this study) suggested a role of these structures in Hh signalling. Here, we characterise cytonemes in two *Drosophila* paradigms, the wing disc and the abdominal epidermis, and investigate their role in Hh gradient formation. We present evidence that cytonemes play an active role in gradient formation: (1) The establishment of the Hh signalling gradient correlates dynamically in space and time with cytoneme formation *in vivo*. (2) Experimental shortening and lengthening of cytonemes affects the gradient accordingly. (3) The analysis of *ttv*$^{-/-}$, *botv*$^{-/-}$ mutant clones implicates cytonemes in Hh transport. Overall, our results support a model in which cytonemes of signal-producing cells are involved in long-range Hh transport (Supplementary Fig. S8).

In wing discs, however, both sending and receiving cells generate cytonemes raising the question which role the cytonemes of receiving cells play. Expression of Ihog in A compartment cells leads to a depletion of Hh from the P compartment cells close to the A/P border[32], which suggests that A compartment cytonemes might actively engage in Hh reception. Hence, cytonemes of both sending and receiving cells might contribute to Hh transport. Interestingly, A compartment cytonemes are rare in histoblasts, suggesting that cytonemes of receiving cells play a minor role in the abdomen.

We observed Ihog-RFP puncta that associated with and moved along cytonemes (Supplementary Video S14). Frequently, such puncta were released from cytonemes (Supplementary Videos S5,S15). We also observed puncta when labelling cytonemes with CD-4-Tomato (Supplementary Video S11). This suggests that cytonemes might transport exovesicles that act as a vehicle for Hh or are the structure where exovesicles are being released. Accordingly, the knock-down of genes involved in exosovesicle production/release has a significant effect on Hh gradient length, and Ihog can be detected in baso-lateral exovesicles at the ultrastructural level. However, the characterisation of these exovesicles as well as their implication in Hh gradient formation requires further analysis. A role of exosomes in morphogen gradient formation has recently been suggested. Active Wnt proteins are secreted in exosomes in cultured cells and in the wing disc[5]. In addition, vesicular release of SonicHh has been implicated in the determination of left-right asymmetry in vertebrates[54]. Very recently, particles containing SonicHh and CDO (the vertebrate homologue of Ihog) that travel along filopodia-like extensions have been described in the chicken limb bud[55].

The mechanisms by which cytonemes could transport morphogens to their targets must ensure specificity and accuracy. One possibility is that cytonemes established contact between sending and receiving cells[9,56]. Alternatively, cytonemes could act as a structure of morphogen release and uptake without cell-cell contacts involved. Our *in vivo* imaging showed that cytonemes are dynamic structures. Cytonemes might grow towards a receiving cell and then retract after a signalling event has taken place, or their dynamics could be determined intrinsically by the stability of their cytoskeleton. Moreover, not just cytoneme length but also their number could shape the gradient, as its brightest section coincides with the dense array of shorter cytonemes. This cytoneme-based model challenges the previous diffusion-based models[57-59] (Supplementary Fig. S8).

Cytonemes have been described in a variety of signalling pathways. The Dpp receptor Thickveins is present in punctate structures moving along cytonemes[60]. Air sac precursors

Europe PMC Funders Author Manuscripts

extend cytonemes towards FGF-expressing cells[61]. Tracheal cells were reported to have at least two types of cytonemes; one type that carries an FGF receptor, and another type that carries the Dpp receptor[9]. This suggests that cytonemes are ligand specific[9]. In the context of Notch signalling, filopodia mediate lateral inhibition between non-neighbouring cells of the pupal notum[56,62]. Interestingly, the dynamic behaviour of these processes is crucial for signalling[56]. Spitz/EGF is delivered through polarised actin protrusions to spatially bias the specification of a particular cell of the *Drosophila* leg[63]. In another example, short cytonemes mediate the delivery of a juxtacrine Hh signal to maintain germ line stem cells in the *Drosophila* ovary[64]. Here, we show that cytonemes also play a pivotal role in long-range Hh signalling in wing disc cells, histoblasts and LECs. Therefore, we believe that cytonemes are a general feature of signalling events of all epithelial cells.

METHODS

Fly mutants

A description of the mutations, insertions and transgenes is available at http://flybase.org. *tub.Gal80^{ts}*, *FLP122* (BDSC, Indiana, USA), *shi^{ts165}* ,*ttv^{524}*, *botv^{51053}*.

Overexpression experiments

The following *Gal4* drivers were used for ectopic expression using the *Gal4/UAS* system[66]: *hh.Gal4*, *ap.Gal4*, *ptc.Gal4*.

The *pUAS*-transgenes were: *UAS.HhGFP*[33], *UAS.Dlp-GFP*[67], *UAS.Disp-YFP*[28], *UAS.Shi^{DN}* [68], *UAS.Ihog*[24], *UAS.Ihog-YFP* and *UAS.Ihog-RFP*[28]. *UAS.Moe-Cherry*[69], *UAS.GPI-YFP*[6], *UAS.GMA*[29], *UAS.RedStinger*, UAS.*CD4-tdTom*[31], *UAS.actin5c-GFP*[70], *UAS.gap43-Venus*[39], *sqh.utrophin-GFP*[36], *Ptc-promotor-trap::GFP* (CB02030; http://flytrap.med.yale.edu), *UAS.SCAR-RNAi* (BDSC 36121), *UAS.Cpa-RNAi* (VDRC v16731), *UAS.Pico-RNAi* (VDRC v16371), *UAS.Flo2-RNAi* (VDRC v31524, v31525), *UAS.TSG101-RNAi* (BDSC 38306), *UAS.Alix-RNAi* (BDSC 33417), *UAS.VPS4-RNAi* (VDRC v105977), *UAS.HRS-RNAi* (BDSC 33900), *UAS.AnxB11-RNAi* (VDRC v101313) *and UAS.Rab11-RNAi* (BDSC 27730). For generating *UAS.Ihog-CFP* the vector pENTR/D-TOPO–Ihog was introduced by recombination into the destination vectors pTWC (pUAS-CFP).

Experimental genotypes and clonal analysis

Transient expression of the *UAS*-constructs using Gal4 drivers and *tub.Gal80^{ts}* was done by keeping the flies at 18°C and inactivate the Gal80^{ts} for 24 to 30 hours at the restrictive temperature (29°C).

Mutant clones were generated by *FLP*-mediated mitotic recombination. Larvae were incubated at 37°C for 1 hour at 24-48 hours after egg laying, or for 45 minutes at 48-72 hours AEL. Flp-out clones in the abdomen were induced for 1 h at 35.5°C. The genotypes of the flies were:

Fig. 3f,g: The transgene *actin>CD2>Gal4*[71] was used to generate ectopic FLP-out clones that expressed *UAS.Disp-YFP*[28] or *UAS.Dlp-GFP*[67].

Fig. 8: *hs.FLP122; FRT42D, ttv^{524}, botv^{510}/FRT42D, FRT42, arm.LacZ; UAS.Ihog-YFP/ hh.Gal4*

Supplementary Fig. S1e,f: *y w hs.FLP122; UAS.RedStinger / If or CyO; UAS.Ihog-RFP / tub<Gal80^{y+}<Gal4.*

Microscopy of imaginal discs

Imaginal discs were fixed in 4% paraformaldehyde (PFA) for 25 min at room temperature (RT) and either imaged directly or used for immunostaining. Exceptions were the wing discs used for the visualisation of cytonemes with the membrane marker *UAS.CD4-tomato* (Fig. 7e-g). These discs were fixed in 4% PFA on ice for 10 min. Cytonemes that did not overexpress Ihog-RFP/CFP were sensitive to fixation. In around 60% of fixed discs that express CD4-Tomato, we observed cytonemes. This might be due to the stabilising effect of Ihog overexpression on cytonemes. A laser scanning confocal microscope (Zeiss LSM510) was used for fluorescence imaging of the discs. ImageJ software (NIH, Bethesda) was used for image processing.

Immunostaining of imaginal discs

Immunostainings were performed according to standard protocols[18]. Antibodies were used at the following dilutions: rabbit polyclonal α-Hh[53] 1/800 and mouse monoclonal α-Ptc (Apa 1.3; Developmental Studies Hybridoma Bank) 1/30. All performed immunostainings were highly reproducible. *n*-numbers of analysed wing discs in each experiment were: Fig. 1a-f, n>200; Fig. 2a, n>50; Fig. 2b, n>25; Fig. 2c, n>200; Fig. 2e, n>25; Fig. 2f, n>50; Fig. 2g, n>25; Fig. 3a, n>200; Fig. 3b,c, n>50; Fig. 3d,e, n>200; Fig. 3f,g, n>20; Fig. 8, n>200.

Immunoelectron microscopy

Larvae were inverted in PBS and fixed in 2% (w/vol) PFA and 0.2% (w/vol) glutaraldehyde in 0.2 M phosphate buffer (PB, pH 7.4) for 2 h at RT and kept in 1% (w/vol) PFA in PB at 4°C. Subsequently, wing discs were dissected, embedded in 10% (w/vol) gelatine, and processed for cryosectioning. Discs were then cut orthogonal to the apical/basal axis on an EM FCS cryo-ultramicrotome (Leica Microsystems) at −120°C. For immunogold labelling, thawed 75-nm thick cryosections were incubated with rabbit α-GFP (1:500, A-6455; Invitrogen) followed by protein A conjugated to 15-nm gold particles (EM Laboratory, Utrecht University, The Netherlands). Sections were stained with a mix of 1.8% methylcellulose and 0,4% uranyl acetate.

In vivo imaging of the abdomen

Pupae were filmed through a window in the pupal case as described[72]. The analysis focused on the dorsal side (tergite) of abdominal segment A2. All imaged flies developed into pharate adults and many hatched. *Z*-stacks of around 40 μm with a step size of 2.5 or 3.0 μm were recorded every 150 or 180 s using a Leica SP5 confocal microscope at 23±2°C. All images and videos shown are projections of *z*-stacks unless stated otherwise. Figures and videos were made using Adobe Illustrator, Adobe Image Ready, Adobe Photoshop, ImageJ (NIH, Bethesda), Volocity (Improvision), and Quicktime Pro (Apple Inc.).

n-numbers of recorded pupae: Video S1, n=10; Video S2, n=10; Video S3, n=11; Video S4, n=3; Video S5, n=7; Videos S6,S7, n=4; Video S8, n=8; Video S9, n=4; Video S10, n=5; Videos S11,S13, n=8; Video S12, n=3; Video S14, n=8; Video S15, n=6.

n-numbers of videos of which frames were used for the Figures: Fig. 4a, n=7; Fig. 4b, n=6; Fig. 4c, n=10; Fig. 4d, n=11; Fig. 4e, n=3; Fig. 4f, n=7; Fig. 5a-c, n=10; Fig. 5d-f, n=4; Fig. 5g, n=8; Fig. 5h, n=4; Fig. 7e'g, n=8; Fig. S1c,d, n=3; Fig. S1e,f, n=4; Fig. S5g, n=3 (Ptc-trap::GFP) and n=5 (Ptc-trap::GFP; Ihog-RFP).

Quantification of cytoneme and gradient length

(1) Gradient length: An area of five cell diameters in height and 120 μm in length, covering the gradient and the A/P border in Ptc-promotor-trap::GFP images, was cropped out to

calculate the 'plot profile' using ImageJ. This procedure plots the vertically averaged pixel intensities along the horizontal axis of the image. Using the 'plot profile' data, the length of the gradient was determined in Microsoft Excel. Gradient length has been defined as the distance from the A/P border up to the point where the gradient 'dipped' below 5% of the maximum fluorescence. We chose this 5% threshold, since at this pixel intensity the signal cannot be clearly distinguished from background noise. We used this 5%-criterion rather than the decay length, because we found that the gradients did not follow an exponential distribution, so that the decay length would not describe the gradient correctly.

(2) Cytoneme reach: To quantify the maximum length of cytonemes, which is the crucial parameter to correlate cytoneme length and gradient length, we measured the length of the two longest protrusions in the wing pouch, from the A/P border to the tip, using the 'line tool' in ImageJ. Then, the average length of the two longest cytonemes was used for the analysis. We used the two longest cytonemes to ensure that we did not use a single outlier for the analysis.

(3) The Kymograph in Fig. 5f was generated using the 'reslice' tool of ImageJ.

Animal models and statistical analysis

All used *Drosophila melanogaster* strains are described above. Third instar larvae and staged pupae were used for the experiments. The sex of the experimental animals was not determined.

All statistical analysis was carried out in R[73] based on a threshold significance level of 0.05. No statistical method was used to predetermine sample sizes. Instead, sample sizes were determined by the available material that we could process during each experiment. No samples have been excluded. The experiments were not randomised. The investigators were only blinded to allocation during the measurement of cytoneme length (Figs. 6,7). To determine the appropriate statistical tests, the data was tested for normal distribution and for equivalence of variance. The following tests, which are justified as appropriate, were conducted:

Tests for treatment effects on cytoneme length (Fig. 7a)—A Kruskal-Wallis test of cytoneme length against the six treatments (*UAS.Ihog-RFP*, *UAS.Pico-RNAi* + *UAS.Ihog-RFP*, *UAS.Cpa-RNAi* + *UAS.Ihog-RFP*, *UAS.Scar-RNAi* + *UAS.Ihog-RFP*, *UAS.Flo2-RNAi* + *UAS.Ihog-RFP* and *UAS.Flo2* + *UAS.Ihog-RFP*) showed a significant effect of treatment (Chi^2=28.84, df=5, P<0.001). Pairwise comparisons using Wilcoxon rank sum tests corrected for multiple comparisons showed significant differences of *UAS.Ihog-RFP* and *UAS.Flo* with each of the 4 *RNAi* treatments (P<0.01 in all cases).

Tests for treatment effects on gradient length (Fig. 7b)—A Kruskal-Wallis test of gradient length against the six treatments (*UAS.Ihog-RFP*, *UAS.Pico-RNAi* + *UAS.Ihog-RFP*, *UAS.Cpa-RNAi* + *UAS.Ihog-RFP*, *UAS.ScarRNAi* + *UAS.Ihog-RFP*, *UAS.Flo2-RNAi* + *UAS.Ihog-RFP* and *UAS.Flo2* + *UAS.Ihog-RFP*) showed a significant effect of treatment (Chi^2=30.03, df=5, P<0.001). Pairwise comparisons using Wilcoxon rank sum tests corrected for multiple comparisons showed significant differences of *UAS.Ihog-RFP* and *UAS.Flo* with each of the 4 *RNAi* treatments (P<0.01 in all cases).

Correlation of gradient length with cytoneme length (Fig. 7c)—Gradient length was significantly positively correlated with cytoneme length for the five treatments and the control (Spearman's rho = 0.89, n = 44 wing discs, P<0.001).

Tests for gradient length with and without Ihog (Fig. 7d)—A Wilcoxon rank sum test of gradient length for the treatments with Ihog (n = 44 wing discs) versus without Ihog (n = 31 wing discs) showed that gradient length was significantly shorter under the Ihog treatments (W = 1074, $P<0.001$). For the six treatments without Ihog overexpression (wild-type, *UAS.Pico-RNAi*, *UAS.Cpa-RNAi*, *UAS.ScarRNAi*, *UAS.Flo2-RNAi* and *UAS.Flo2*), a Kruskal-Wallis test showed a significant effect of treatment on gradient length ($Chi^2=25.42$, df=5, $P<0.001$). Wilcoxon rank sum tests corrected for multiple comparisons showed significant differences of wild-type and *UAS.Flo2* with each of the 4 *RNAi* treatments ($P<0.05$ in all cases).

Correlation of gradient length with cytoneme length for CD4-Tomato (Fig. 7f') —Using the CD4-Tomato expression to visualise cytonemes, there was a significant positive correlation between gradient length and cytoneme length (Spearman's rho = 0.78, n=14 wing discs, $P<0.01$).

Tests for treatment effects on gradient length related to exosome production (Supplementary Fig. S7e)—Analysis of variance of ln (gradient length) against treatment for the seven treatments related to exosome production (wild-type, *UAS.TSG101-RNAi*, *UAS.VPS4-RNAi*, *UAS.HRS-RNAi*, *UAS.AnxB11-RNAi*, *UAS.Alix-RNAi*, *UAS.Rab11-RNAi*) showed a significant effect of treatment ($F_{6,67}=4.83$, $P<0.001$). Tukey's Honest Significant Difference tests showed that confidence intervals did not overlap for wild-type with the RNAi treatments ($P<0.05$ in all cases).

Supplementary Material

Refer to Web version on PubMed Central for supplementary material.

Acknowledgments

We are grateful to P. Lawrence in whose lab the abdomen work has been done. We also thank T. Kornberg for helpful insights, V. Dietrich-Bischoff, P. Lawrence and C. Delidakis for helpful comments on the manuscript, T. Tabata for α-Hh antibody, X. Lin for Dlp-GFP flies, and BDSC and VDRC for stocks. R. Wilson assisted with statistical analysis. C. Ibañez, and V. Sánchez in IG lab contributed to RNAi screening. We also thank Milagros Guerra at the EM Unit and the confocal microscopy service of the Centro de Biología Molecular "Severo Ochoa," as well as the confocal facility of the Department of Zoology – which is funded by the Wellcome Trust and the Isaac Newton Trust – for skilful technical assistance. Work was supported by grants BFU2008-03320/BMC, BFU2011-25987 and Consolider Program CDS 2007-00008 from the Spanish MICINN, by Marie Curie FP7 (ITN 238186) and by an institutional grant from the *Fundación Areces*. IS was supported by a FPI fellowship from the Spanish MICINN, ACG by a Marie Curie ITN FP7 contract, GA by the Amarouto Program for senior researchers from the Comunidad Autónoma de Madrid and grant BFU2009-08085 from the Spanish MICINN, and MB by Project Grant WG086986 and Senior Investigator Award WT096645MA by the Wellcome Trust to P. Lawrence.

REFERENCES

1. Lawrence PA. Morphogens: how big is the big picture? Nat Cell Biol. 2001; 3:E151–154. [PubMed: 11433305]
2. Gradilla AC, Guerrero I. Hedgehog on the move: a precise spatial control of Hedgehog dispersion shapes the gradient. Curr Opin Genet Dev. 2013 doi:10.1016/j.gde.2013.04.011.
3. Crick F. Diffusion in embryogenesis. Nature. 1970; 225:420–422. [PubMed: 5411117]
4. Entchev EV, Schwabedissen A, Gonzalez-Gaitan M. Gradient formation of the TGF-beta homolog Dpp. Cell. 2000; 103:981–991. [PubMed: 11136982]
5. Gross JC, Chaudhary V, Bartscherer K, Boutros M. Active Wnt proteins are secreted on exosomes. Nat Cell Biol. 2012; 14:1036–1045. [PubMed: 22983114]
6. Greco V, Hannus M, Eaton S. Argosomes: a potential vehicle for the spread of morphogens through epithelia. Cell. 2001; 106:633–645. [PubMed: 11551510]

7. Panakova D, Sprong H, Marois E, Thiele C, Eaton S. Lipoprotein particles are required for Hedgehog and Wingless signalling. Nature. 2005; 435:58–65. [PubMed: 15875013]
8. Ramirez-Weber FA, Kornberg TB. Cytonemes: cellular processes that project to the principal signaling center in *Drosophila* imaginal discs. Cell. 1999; 97:599–607. [PubMed: 10367889]
9. Roy S, Hsiung F, Kornberg TB. Specificity of *Drosophila* cytonemes for distinct signaling pathways. Science. 2011; 332:354–358. [PubMed: 21493861]
10. Ingham PW, Nakano Y, Seger C. Mechanisms and functions of Hedgehog signalling across the metazoa. Nat Rev Genet. 2011; 12:393–406. [PubMed: 21502959]
11. Porter JA, Young KE, Beachy PA. Cholesterol modification of hedgehog signaling proteins in animal development. Science. 1996; 274:255–259. [PubMed: 8824192]
12. Pepinsky RB, et al. Identification of a palmitic acid-modified form of human Sonic hedgehog. J Biol Chem. 1998; 273:14037–14045. [PubMed: 9593755]
13. Strigini M, Cohen SM. A Hedgehog activity gradient contributes to AP axial patterning of the *Drosophila* wing. Development. 1997; 124:4697–4705. [PubMed: 9409685]
14. Mullor JL, Calleja M, Capdevila J, Guerrero I. Hedgehog activity, independent of decapentaplegic, participates in wing disc patterning. Development. 1997; 124:1227–1237. [PubMed: 9102309]
15. Garcia-Bellido A, Ripoll P, Morata G. Developmental compartmentalisation of the wing disk of *Drosophila*. Nat New Biol. 1973; 245:251–253. [PubMed: 4518369]
16. Tabata T, Kornberg TB. Hedgehog is a signaling protein with a key role in patterning *Drosophila* imaginal discs. Cell. 1994; 76:89–102. [PubMed: 8287482]
17. Porter JA, et al. The product of hedgehog autoproteolytic cleavage active in local and long-range signalling. Nature. 1995; 374:363–366. [PubMed: 7885476]
18. Capdevila J, Estrada MP, Sanchez-Herrero E, Guerrero I. The *Drosophila* segment polarity gene patched interacts with decapentaplegic in wing development. EMBO J. 1994; 13:71–82. [PubMed: 8306973]
19. Chen Y, Struhl G. Dual roles for patched in sequestering and transducing Hedgehog. Cell. 1996; 87:553–563. [PubMed: 8898207]
20. Struhl G, Barbash DA, Lawrence PA. Hedgehog organises the pattern and polarity of epidermal cells in the *Drosophila* abdomen. Development. 1997; 124:2143–2154. [PubMed: 9187141]
21. Kopp A, Muskavitch MA, Duncan I. The roles of hedgehog and engrailed in patterning adult abdominal segments of *Drosophila*. Development. 1997; 124:3703–3714. [PubMed: 9367426]
22. Kopp A, Duncan I. Anteroposterior patterning in adult abdominal segments of *Drosophila*. Dev Biol. 2002; 242:15–30. [PubMed: 11795937]
23. Madhavan MM, Madhavan K. Morphogenesis of the epidermis of adult abdomen of *Drosophila*. J Embryol Exp Morphol. 1980; 60:1–31. [PubMed: 6796636]
24. Zheng X, Mann RK, Sever N, Beachy PA. Genetic and biochemical definition of the Hedgehog receptor. Genes Dev. 2010; 24:57–71. [PubMed: 20048000]
25. Yao S, Lum L, Beachy P. The ihog cell-surface proteins bind Hedgehog and mediate pathway activation. Cell. 2006; 125:343–357. [PubMed: 16630821]
26. Yan D, et al. The cell-surface proteins Dally-like and Ihog differentially regulate Hedgehog signaling strength and range during development. Development. 2010; 137:2033–2044. [PubMed: 20501592]
27. Kim MS, Saunders AM, Hamaoka BY, Beachy PA, Leahy DJ. Structure of the protein core of the glypican Dally-like and localization of a region important for hedgehog signaling. PNAS. 2011; 108:13112–13117. [PubMed: 21828006]
28. Callejo A, et al. Dispatched mediates Hedgehog basolateral release to form the long-range morphogenetic gradient in the *Drosophila* wing disk epithelium. PNAS. 2011; 108:12591–12598. [PubMed: 21690386]
29. Bloor JW, Kiehart DP. zipper Nonmuscle myosin-II functions downstream of PS2 integrin in *Drosophila* myogenesis and is necessary for myofibril formation. Dev Biol. 2001; 239:215–228. [PubMed: 11784030]
30. Langhorst MF, Reuter A, Stuermer CA. Scaffolding microdomains and beyond: the function of reggie/flotillin proteins. Cell Mol Life Sci. 2005; 62:2228–2240. [PubMed: 16091845]

31. Han C, Jan LY, Jan YN. Enhancer-driven membrane markers for analysis of nonautonomous mechanisms reveal neuron-glia interactions in *Drosophila*. PNAS. 2011; 108:9673–9678. [PubMed: 21606367]
32. Bilioni A, et al. Balancing Hedgehog, a retention and release equilibrium given by Dally, Ihog, Boi and shifted/DmWif. Dev Biol. 2013; 376:198–212. [PubMed: 23276604]
33. Torroja C, Gorfinkiel N, Guerrero I. Patched controls the Hedgehog gradient by endocytosis in a dynamin-dependent manner, but this internalization does not play a major role in signal transduction. Development. 2004; 131:2395–2408. [PubMed: 15102702]
34. Burke R, et al. Dispatched, a novel sterol-sensing domain protein dedicated to the release of cholesterol-modified hedgehog from signaling cells. Cell. 1999; 99:803–815. [PubMed: 10619433]
35. Lum L, et al. Identification of Hedgehog pathway components by RNAi in *Drosophila* cultured cells. Science. 2003; 299:2039–2045. [PubMed: 12663920]
36. Rauzi M, Lenne PF, Lecuit T. Planar polarized actomyosin contractile flows control epithelial junction remodelling. Nature. 2010; 468:1110–1114. [PubMed: 21068726]
37. Mallavarapu A, Mitchison T. Regulated actin cytoskeleton assembly at filopodium tips controls their extension and retraction. J Cell Biol. 1999; 146:1097–1106. [PubMed: 10477762]
38. Lee K, Gallop JL, Rambani K, Kirschner MW. Self-assembly of filopodia-like structures on supported lipid bilayers. Science. 2010; 329:1341–1345. [PubMed: 20829485]
39. Mavrakis M, Rikhy R, Lippincott-Schwartz J. Plasma membrane polarity and compartmentalization are established before cellularization in the fly embryo. Dev Cell. 2009; 16:93–104. [PubMed: 19154721]
40. Cooper JA, Sept D. New insights into mechanism and regulation of actin capping protein. Int Rev Cell Mol Biol. 2008; 267:183–206. [PubMed: 18544499]
41. Delalle I, Pfleger CM, Buff E, Lueras P, Hariharan IK. Mutations in the *Drosophila* orthologs of the F-actin capping protein alpha- and beta-subunits cause actin accumulation and subsequent retinal degeneration. Genetics. 2005; 171:1757–1765. [PubMed: 16143599]
42. Uruno T, Remmert K, Hammer JA 3rd. CARMIL is a potent capping protein antagonist: identification of a conserved CARMIL domain that inhibits the activity of capping protein and uncaps capped actin filaments. J Biol Chem. 2006; 281:10635–10650. [PubMed: 16434392]
43. Chhabra ES, Higgs HN. The many faces of actin: matching assembly factors with cellular structures. Nat Cell Biol. 2007; 9:1110–1121. [PubMed: 17909522]
44. Kunda P, Craig G, Dominguez V, Baum B. Abi, Sra1, and Kette control the stability and localization of SCAR/WAVE to regulate the formation of actin-based protrusions. Curr Biol. 2003; 13:1867–1875. [PubMed: 14588242]
45. Rogers SL, Wiedemann U, Stuurman N, Vale RD. Molecular requirements for actin-based lamella formation in *Drosophila* S2 cells. J Cell Biol. 2003; 162:1079–1088. [PubMed: 12975351]
46. Georgiou M, Baum B. Polarity proteins and Rho GTPases cooperate to spatially organise epithelial actin-based protrusions. J Cell Sci. 2010; 123:1089–1098. [PubMed: 20197404]
47. Lyulcheva E, et al. *Drosophila* pico and its mammalian ortholog lamellipodin activate serum response factor and promote cell proliferation. Dev Cell. 2008; 15:680–690. [PubMed: 19000833]
48. Neumann-Giesen C, et al. Membrane and raft association of reggie-1/flotillin-2: role of myristoylation, palmitoylation and oligomerization and induction of filopodia by overexpression. Biochem J. 2004; 378:509–518. [PubMed: 14599293]
49. Katanaev VL, et al. Reggie-1/flotillin-2 promotes secretion of the long-range signalling forms of Wingless and Hedgehog in *Drosophila*. EMBO J. 2008; 27:509–521. [PubMed: 18219274]
50. Raposo G, Stoorvogel W. Extracellular vesicles: exosomes, microvesicles, and friends. J Cell Biol. 2013; 200:373–383. [PubMed: 23420871]
51. Rusten TE, Vaccari T, Stenmark H. Shaping development with ESCRTs. Nat Cell Biol. 2012; 14:38–45. [PubMed: 22193162]
52. Bellaiche Y, The I, Perrimon N. Tout-velu is a *Drosophila* homologue of the putative tumour suppressor EXT-1 and is needed for Hh diffusion. Nature. 1998; 394:85–88. [PubMed: 9665133]

53. Takei Y, Ozawa Y, Sato M, Watanabe A, Tabata T. Three *Drosophila* EXT genes shape morphogen gradients through synthesis of heparan sulfate proteoglycans. Development. 2004; 131:73–82. [PubMed: 14645127]
54. Tanaka Y, Okada Y, Hirokawa N. FGF-induced vesicular release of Sonic hedgehog and retinoic acid in leftward nodal flow is critical for left-right determination. Nature. 2005; 435:172–177. [PubMed: 15889083]
55. Sanders TA, Llagostera E, Barna M. Specialized filopodia direct long-range transport of SHH during vertebrate tissue patterning. Nature. 2013; 497:628–632. [PubMed: 23624372]
56. Cohen M, Georgiou M, Stevenson NL, Miodownik M, Baum B. Dynamic filopodia transmit intermittent Delta-Notch signaling to drive pattern refinement during lateral inhibition. Dev Cell. 2010; 19:78–89. [PubMed: 20643352]
57. Zeng X, et al. A freely diffusible form of Sonic hedgehog mediates long-range signalling. Nature. 2001; 411:716–720. [PubMed: 11395778]
58. Lander AD, Nie Q, Wan FY. Do morphogen gradients arise by diffusion? Dev Cell. 2002; 2:785–796. [PubMed: 12062090]
59. Saha K, Schaffer DV. Signal dynamics in Sonic hedgehog tissue patterning. Development. 2006; 133:889–900. [PubMed: 16452094]
60. Hsiung F, Ramirez-Weber FA, Iwaki DD, Kornberg TB. Dependence of *Drosophila* wing imaginal disc cytonemes on Decapentaplegic. Nature. 2005; 437:560–563. [PubMed: 16177792]
61. Sato M, Kornberg TB. FGF is an essential mitogen and chemoattractant for the air sacs of the drosophila tracheal system. Dev Cell. 2002; 3:195–207. [PubMed: 12194851]
62. De Joussineau C, et al. Delta-promoted filopodia mediate long-range lateral inhibition in *Drosophila*. Nature. 2003; 426:555–559. [PubMed: 14654840]
63. Peng Y, Han C, Axelrod JD. Planar polarized protrusions break the symmetry of EGFR signaling during *Drosophila* bract cell fate induction. Dev Cell. 23:507–518. [PubMed: 22921201]
64. Rojas-Rios P, Guerrero I, Gonzalez-Reyes A. Cytoneme-mediated delivery of hedgehog regulates the expression of bone morphogenetic proteins to maintain germline stem cells in *Drosophila*. PLoS Biol. 2012; 10:e1001298. [PubMed: 22509132]
65. Grigliatti TA, Hall L, Rosenbluth R, Suzuki DT. Temperature-sensitive mutations in *Drosophila* melanogaster. XIV. A selection of immobile adults. Mol Gen Genet. 1973; 120:107–114. [PubMed: 4631264]
66. Brand AH, Perrimon N. Targeted gene expression as a means of altering cell fates and generating dominant phenotypes. Development. 1993; 118:401–415. [PubMed: 8223268]
67. Han C, Belenkaya TY, Wang B, Lin X. *Drosophila* glypicans control the cell-to-cell movement of Hedgehog by a dynamin-independent process. Development. 2004; 131:601–611. [PubMed: 14729575]
68. Moline MM, Southern C, Bejsovec A. Directionality of wingless protein transport influences epidermal patterning in the *Drosophila* embryo. Development. 1999; 126:4375–4384. [PubMed: 10477304]
69. Millard TH, Martin P. Dynamic analysis of filopodial interactions during the zippering phase of *Drosophila* dorsal closure. Development. 2008; 135:621–626. [PubMed: 18184725]
70. Roper K, Mao Y, Brown NH. Contribution of sequence variation in *Drosophila* actins to their incorporation into actin-based structures in vivo. J Cell Sci. 2005; 118:3937–3948. [PubMed: 16105877]
71. Pignoni F, Zipursky SL. Induction of *Drosophila* eye development by decapentaplegic. Development. 1997; 124:271–278. [PubMed: 9053304]
72. Bischoff M, Cseresnyes Z. Cell rearrangements, cell divisions and cell death in a migrating epithelial sheet in the abdomen of *Drosophila*. Development. 2009; 136:2403–2411. [PubMed: 19542353]
73. R Development Core Team. R: A language and environment for statistical computing. R Foundation for Statistical Computing; Vienna, Austria: 2011.

Europe PMC Funders Author Manuscripts

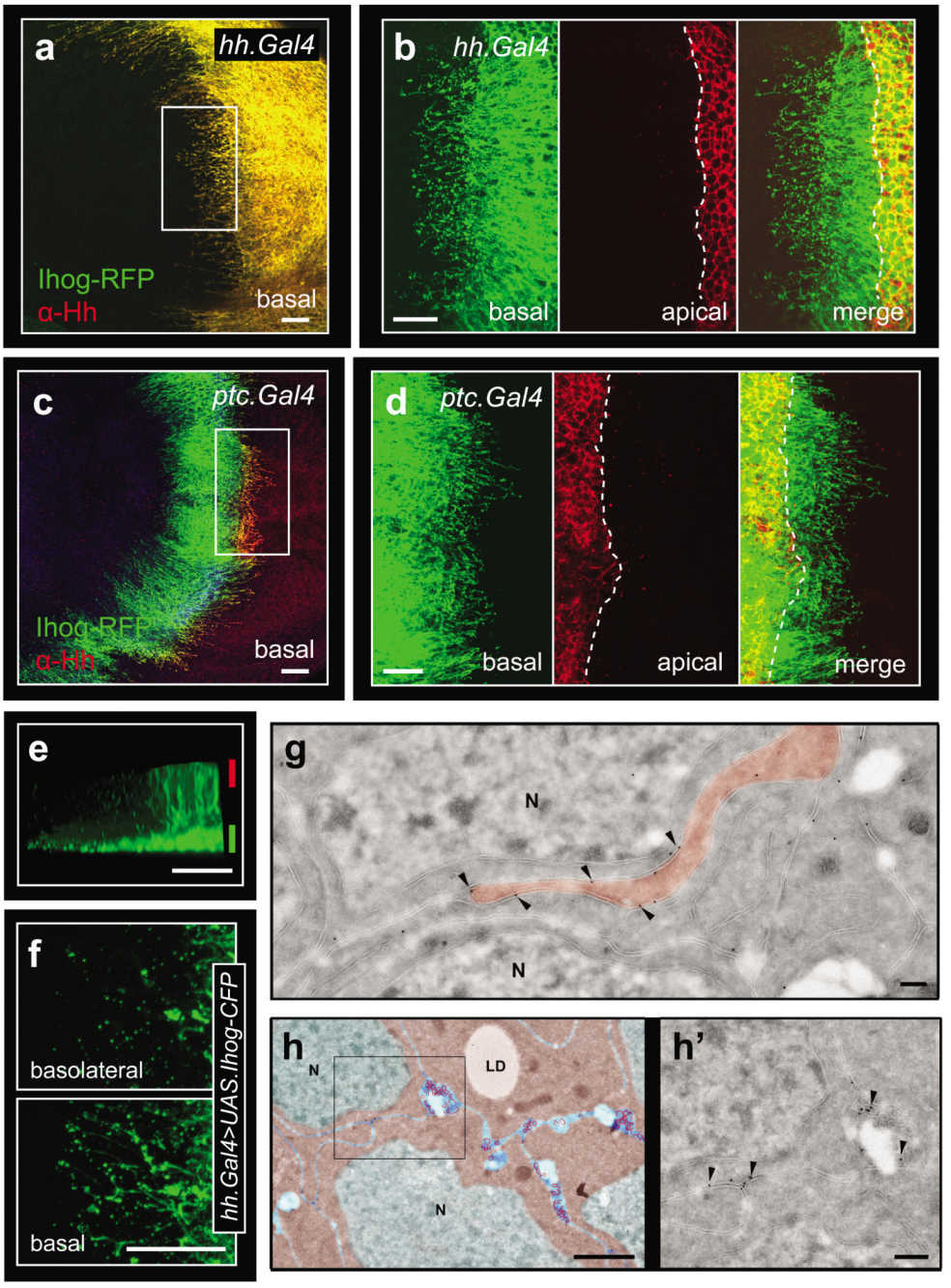

Figure 1. Wing disc cells generate actin-based basal cytonemes.

Fluorescently labelled Ihog marks cytonemes in both the A and the P compartment. Bars, 20 μm. White dotted lines indicate A/P boundaries. (**a**,**b**) *hh.Gal4>UAS.Ihog-RFP* discs, co-labelled with α-Hh antibody. (**a**) Overview of a basal *z*-section showing P compartment cytonemes that point anteriorly into the A compartment. (**b**) Detail of the region highlighted in (a). (**c**,**d**) *ptc.Gal4>UAS.Ihog-RFP* discs, co-labelled with α-Hh antibody. (**c**) Overview of a basal *z*-section showing A compartment cytonemes that point posteriorly into the P compartment. Note that protrusions also point anteriorly. (**d**) Detail of the region highlighted in (c). Like P compartment cells (b), A compartment cells show a dense array of shorter

protrusions reaching into the neighbouring compartment as well as individual longer protrusions. (**e**) Cytonemes are basal structures. Lateral view of the P compartment cells shown in (b). Red and green bars indicate apical and basal sections, respectively. (**f**) Ihog-CFP labels punctate structures that not only decorate basal cytonemes, but are also found basolaterally, without being associated to cytonemes. (**g,h**) Immunoelectron microscopy of the Ihog protein in *hh.Gal4/UAS.Ihog-CFP* wing disc cryosections. Immunogold labelling was performed with an anti-GFP antibody followed by protein A conjugated to 15-nm gold particles (n=9 cryosections). **(g)** Ihog labelling at the basolateral membrane of a thin cytoplasmic protrusion (depicted in brown). **(h)** Ihog staining at basolateral membranes and exovesicles. Nuclei (green), cytoplasm (brown), extracellular space (blue) and exovesicles (red) are depicted by colours. **(h')** Detail of the area delimited in (h). Arrowheads indicate gold particles on membranes and exovesicles; N, nucleus; LD, lipid droplet; Bars, 200 nm (g,h'), 1 μm (h). In all figures, anterior is to the left.

Europe PMC Funders Author Manuscripts

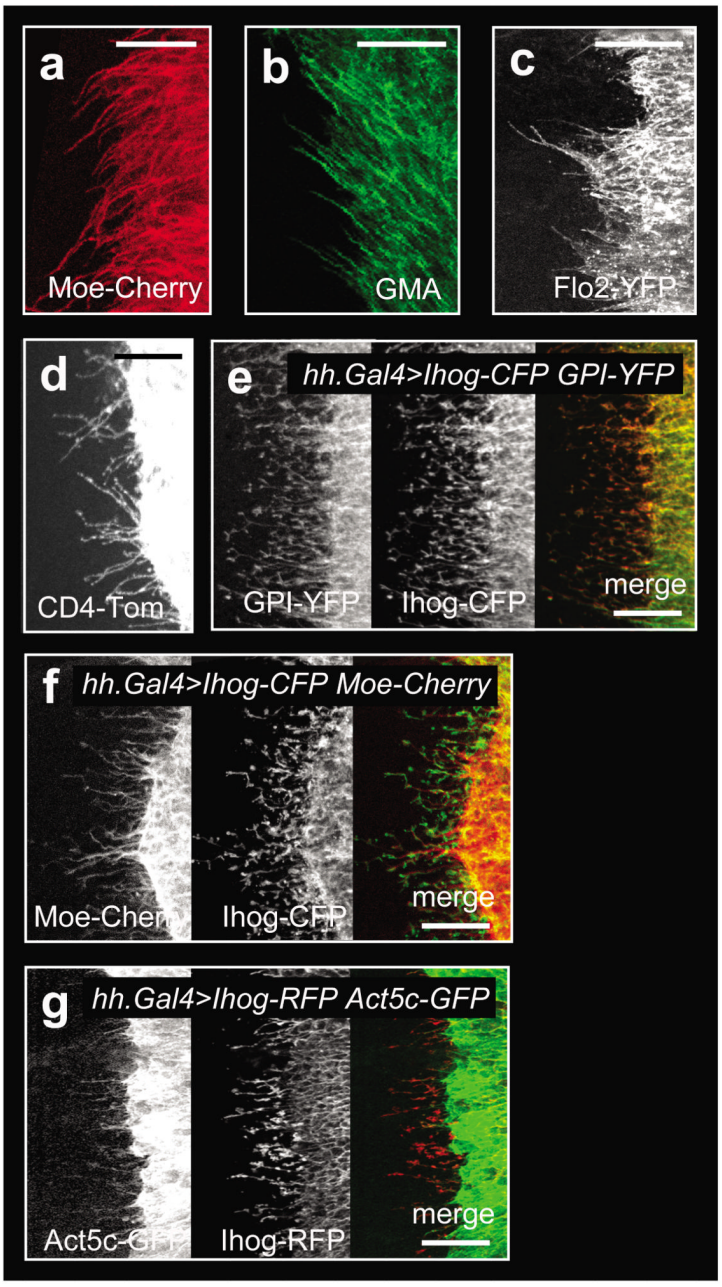

Figure 2. Cytoskeletal and membrane markers label cytonemes in the wing disc.

Cytonemes are labelled by actin cytoskeletal markers Moe-Cherry (**a**) and GMA (**b**) as well as by membrane markers Flo2-YFP (**c**) CD4-Tomato (**d**) and GPI-YFP (co-expressed with Ihog-CFP) (**e**), all driven by *hh.Gal4*. Note that GPI-YFP and Ihog-CFP colocalise. (**f,g**) Expression of Ihog stabilises cytonemes. Compared to the expression of cytoskeletal markers alone (a,b), co-expression of IHog-CFP and Moe-Cherry (**f**) as well as of Ihog-RFP and Act5c-GFP (**g**) increases visibility and number of cytonemes. Note that Moe-Cherry and Actin5c-GFP only label cytonemes, but not the dotted structures seen with Ihog. Bars, 20 μm.

Europe PMC Funders Author Manuscripts

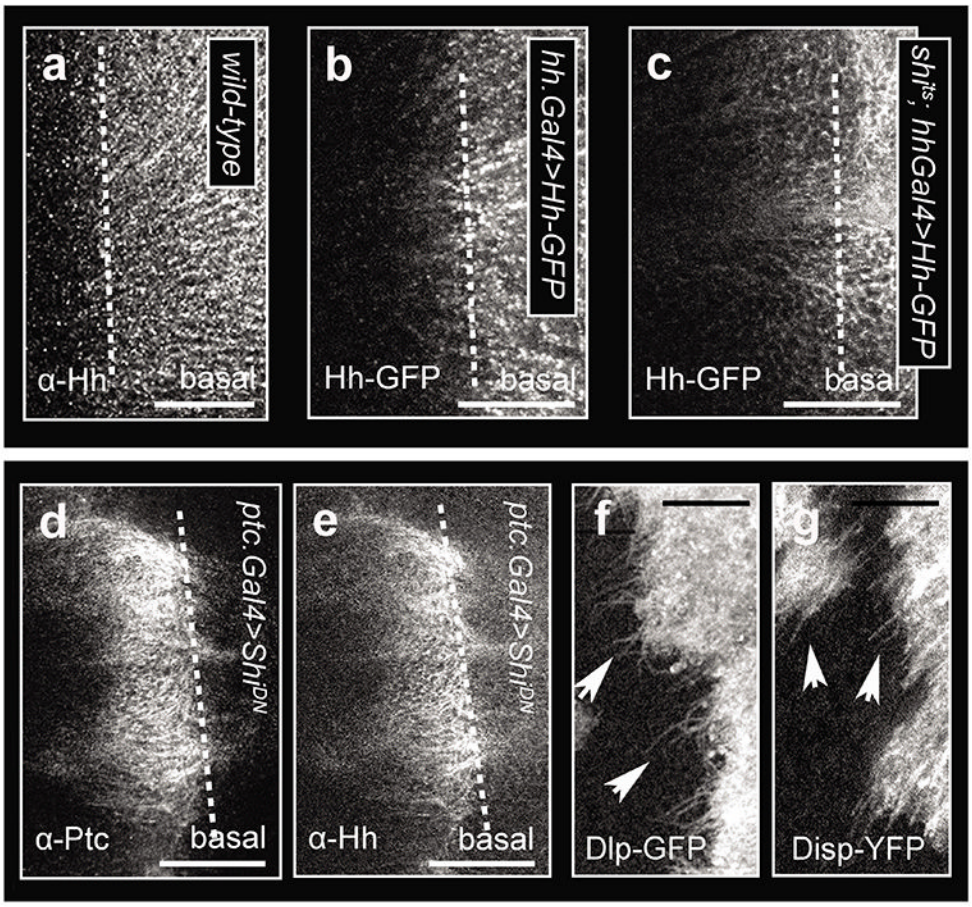

Figure 3. Components of the Hh pathway are associated to cytonemes in wing discs.

Endogenous Hh (**a**) and ectopic Hh-GFP driven by *hh.Gal4* (**b**) can be observed in puncta that appear to be organised in threads and reach into the A compartment. (**c**) 'Freezing endocytosis' in *shi*^{ts} mutants increases the visibility of Hh-GFP in cytonemes. *shi*^{ts}*, hh.Gal4>UAS.Hh-GFP* wing disc shown after one hour at restrictive temperature. (**d**,**e**) 'Freezing endocytosis' in the receiving cells by expressing *ptc.Gal4>UAS.shi*^{DN}*, tub.Gal80ts* increases visibility of endogenous Ptc (**d**) and Hh (**e**) in puncta. These puncta appear to be organised in threads and reach into the P compartment. Wing disc shown after 14 hours at restrictive temperature. (**f**,**g**) Both Dlp-GFP (**f**) and Disp-YFP (**g**), expressed in clones of cells, label cytonemes (arrows). Dotted lines indicate A/P boundaries. Bars, 20 μm.

Europe PMC Funders Author Manuscripts

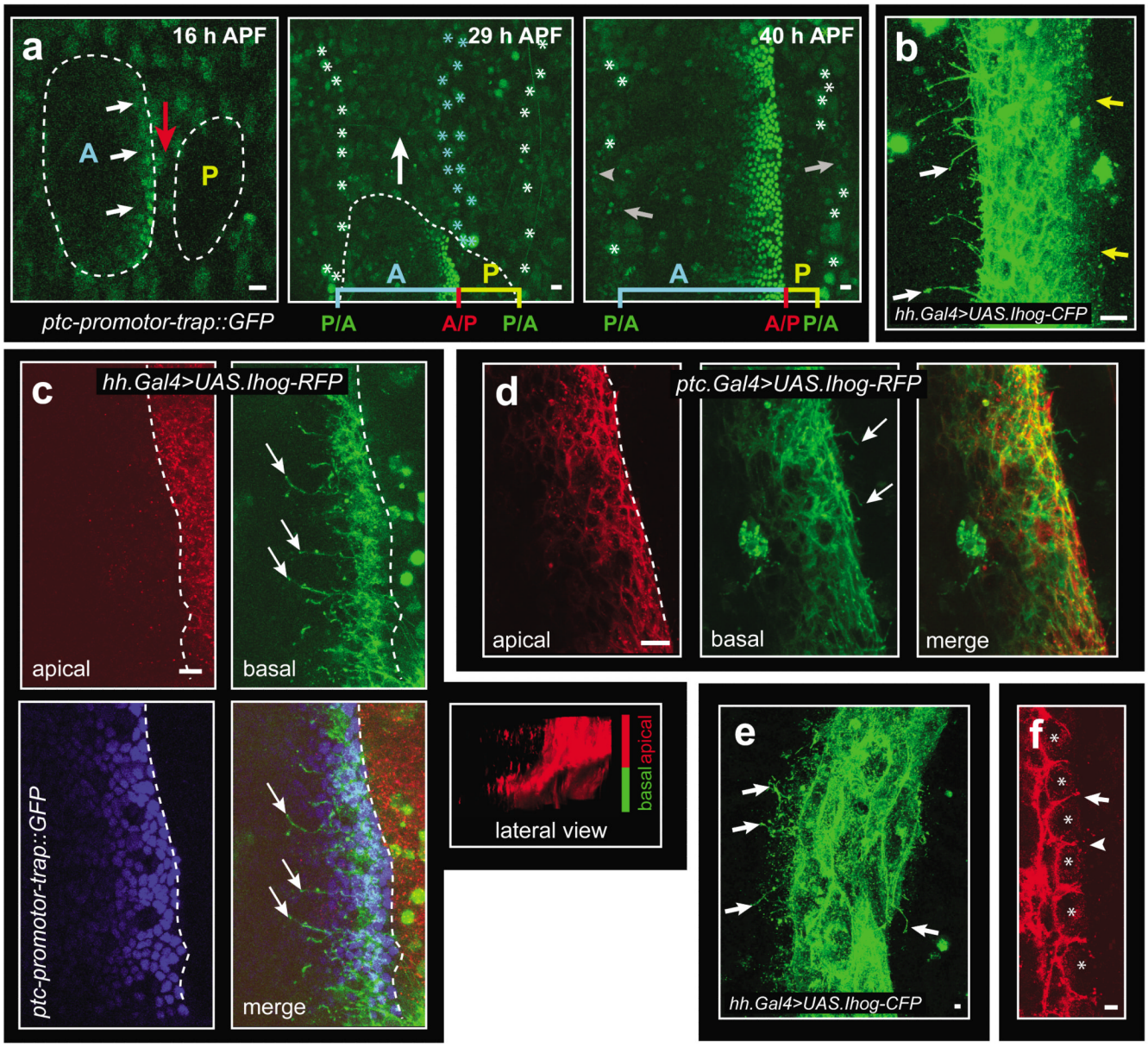

Figure 4. Hh signalling and cytonemes in the abdominal epidermis.

(**a**) Hh signalling as reported by Ptc-promotor-trap::GFP. Early stage (left): ADH and PDH nests still separated by a row of LECs (red arrow). In the ADH nest, the reporter is switched on faintly in a few cells (white arrows). 'Intermediate' stage (middle): The histoblast mass (hatched line) moves in dorsal direction (arrow) and replaces LECs. A row of A compartment LECs posterior to the P compartment expresses Ptc-promotor-trap::GFP (white asterisks). Furthermore, A compartment LECs anterior to the P compartment express the reporter (cyan asterisks). In histoblasts, Ptc-promotor-trap::GFP shows graded expression anterior to the A/P border. Late stage (right): adult epithelium almost formed. Graded reporter expression visible anterior to the A/P border in histoblasts. Furthermore, reporter expression starts in histoblast regions where neighbouring segments touch (grey arrows). LECs still present at segment boundaries also express GFP (asterisks). Cyan and yellow lines indicate A and P compartments, respectively. Red line indicates A/P border. See

Supplementary Fig. S1 for scheme. (**b**) P compartment cells display cytonemes in anterior (white arrows) but not posterior (yellow arrows) direction into the A compartments. *hh.Gal4>UAS.Ihog-CFP* labels cells at end of abdominal closure. (**c**) P compartment cytonemes are basal and reach far into the A compartment, covering the Ptc-promotor-trap::GFP gradient. Note dense array of shorter protrusions and individual longer protrusions (white arrows). *hh.Gal4>UAS.Ihog-RFP* labels P compartment cells, and Ptc-promotor-trap::GFP labels A compartment cells responding to Hh. Small box shows lateral view. (**d**) Cytonemes of A compartment cells (white arrows) are rare and shorter than those of P compartment cells. *ptc.Gal4>UAS.Ihog-RFP* labels cells. (**e**) P compartment LECs display cytonemes mainly in anterior but also posterior direction (white arrows) during their posterior migration phase. *hh.Gal4>UAS.Ihog-CFP* labels cells. See Supplementary Video S4. (**f**) When morphogenetic process begins (around 15 h APF), P compartment LECs generate cytonemes (arrow) that 'surround' LECs of first row of neighbouring segment (asterisks) – these A compartment LECs also begin to express *ptc-promotor-trap::GFP* (Supplementary Video S2). At the tip of the protrusions, vesicles emanate (arrowhead). *hh.Gal4>UAS.Ihog-CFP* labels LECs. See Supplementary Video S5. White hatched line indicates A/P border in (c,d). Bars, 10 μm.

Europe PMC Funders Author Manuscripts

Europe PMC Funders Author Manuscripts

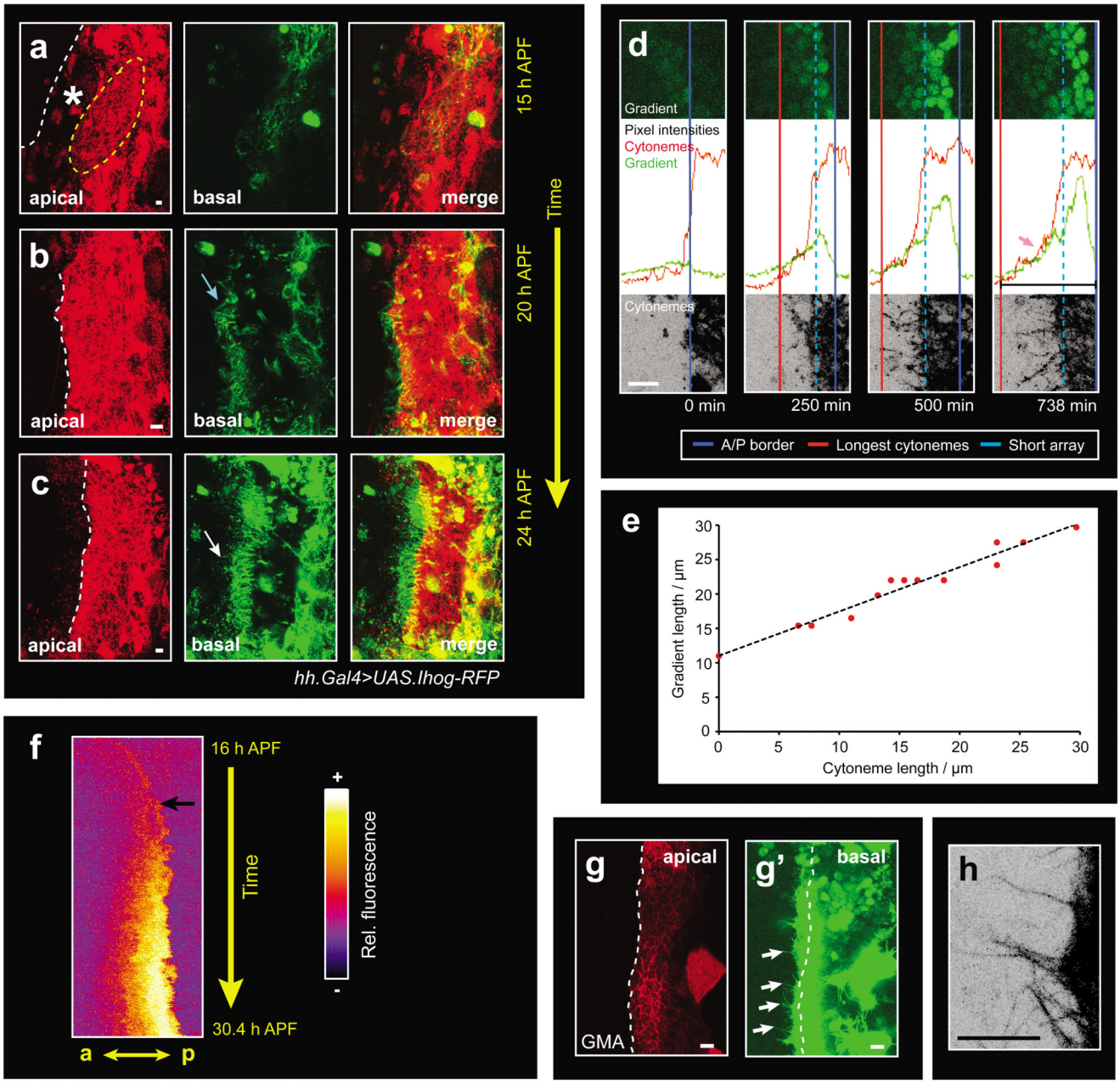

Figure 5. Cytonemes behave dynamically, and their development correlates with Hh signalling gradient establishment.

(**a-c**) Cytonemes develop over time. *hh.Gal4>UAS.Ihog-RFP* labels P compartment cells. (**a**) No cytonemes observed before ADH and PDH nests fuse. Yellow hatched line outlines PDH nest; asterisk indicates LECs separating ADH and PDH nests. (**b**) After nest fusion, basal cytonemes start to form (cyan arrow). (**c**) Four hours later, cytonemes fully developed - note dense array of shorter protrusions and prominent longer protrusions (white arrow). See Supplementary Video S2. (**d-f**) Cytoneme development correlates with gradient formation. *hh.Gal4>UAS.Ihog-RFP* labels P compartment cytonemes; Ptc-promotor-trap::GFP indicates Hh activity gradient. (**d**) Four frames from Supplementary Video S7. Top panels – Hh activity gradient shown by expression of the Ptc-promotor-trap::GFP.

Europe PMC Funders Author Manuscripts

Bottom panels – cytonemes in a basal section of Ihog-RFP channel. Middle panels – profile plots of vertically averaged pixel intensities for panels above (green curve) and below (red curve). Blue line marks A/P border. 0 min: ADH and PDH nest fusion, no cytonemes present. 738 min: End of video, cytonemes present, and gradient established. Maximum cytoneme length (red line) correlates with gradient width (black line). The Hh activity gradient (green curve) and cytoneme density along the a-p axis (red curve) also correlate: the short array (cyan dotted line) coincides with the brightest gradient section, both curves decline similarly (pink arrow). This relation is already visible during gradient formation (two centre frames). (**e**) Gradient length correlates with maximum cytoneme length over time. (**f**) Kymograph illustrating establishment of the Ptc-promotor-trap::GFP gradient over time. Pixel intensities per time point for Supplementary Video S6 (top panel, 2.5 min intervals) were vertically averaged. The resulting horizontal lines were then plotted along the *y*-axis, illustrating change in fluorescence over time. Black arrow indicates time when ADH and PDH nests fuse. (**g**,**h**) P compartment cytonemes labelled with the actin cytoskeleton marker GMA driven by *hh.Gal4*. (**g**,**g**') *A*pical (red) and basal (green) *z*-sections. Some cytonemes indicated with white arrows. (**h**) Close-up of individual cytonemes labelled with GMA. See Supplementary Video S9. White hatched lines indicate A/P border. Bars, 10 μm.

Europe PMC Funders Author Manuscripts

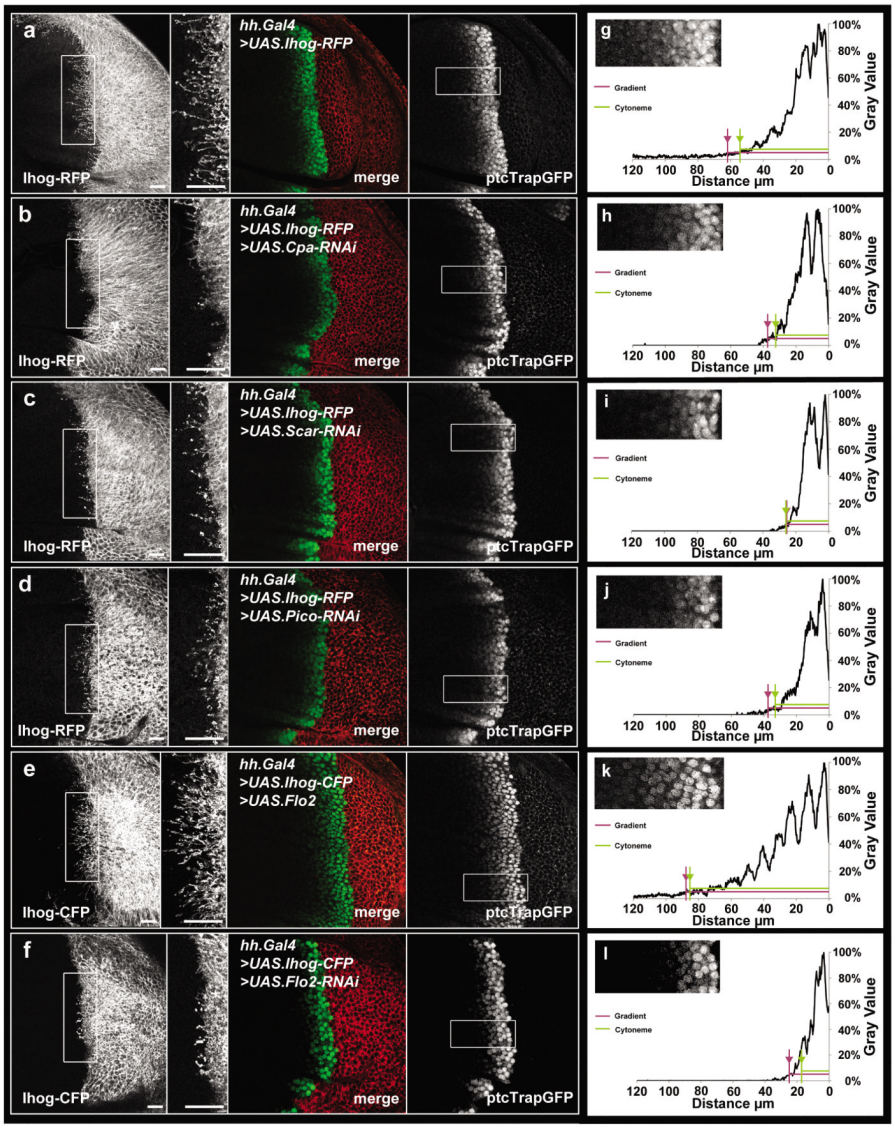

Figure 6. Interfering with cytoneme length affects the Hh activity gradient.

(**a-f**) Fluorescence images of wing discs, in which the cytonemes are labelled with *hh.Gal4>UAS.Ihog-RFP* (left panel; detail shown in the adjacent panel) and the Hh activity gradient is visualised using Ptc-promotor-trap::GFP (right panel). The merge of both channels is shown in the centre. In addition, *RNAi*- or *UAS*-constructs were co-expressed in the P compartment to interfere with cytoneme formation. (**a**) Control comprising Ihog-RFP only. (**b**) *Cpa-RNAi* and Ihog-RFP. (**c**) *Scar-RNAi* and Ihog-RFP. (**d**) *Pico-RNAi* and Ihog-RFP. (**e**) *UAS.Flo2* and Ihog-CFP. (**f**) *Flo2-RNAi* and *Ihog-YFP*. In the RNAi wing discs (b-d,f), both the cytonemes and the gradient are shorter than in the control (a). In *UAS.Flo2* wing discs (e), cytonemes and gradient are longer than in the control (a). (**g-l**) Quantification of gradient length in the wing discs shown in (a-f) using profile plots. The graphs depict the vertically averaged pixel intensities along the horizontal (a-p) axis of the detail of the Ptc-promotor-trap::GFP image shown in the top left corner. The red arrows indicate the length of the gradient, up to the point where the average pixel intensity drops below 5% of the maximum intensity. The green arrows show the average length of the two longest cytonemes in the analysed disc. These parameters have been chosen to determine cytoneme reach and

gradient length in our fixed samples as accurately as possible (see Methods for further information). However, this quantification has its limitations, since the parameters have been chosen to some extent arbitrarily. Bars, 20 μm.

Europe PMC Funders Author Manuscripts

Europe PMC Funders Author Manuscripts

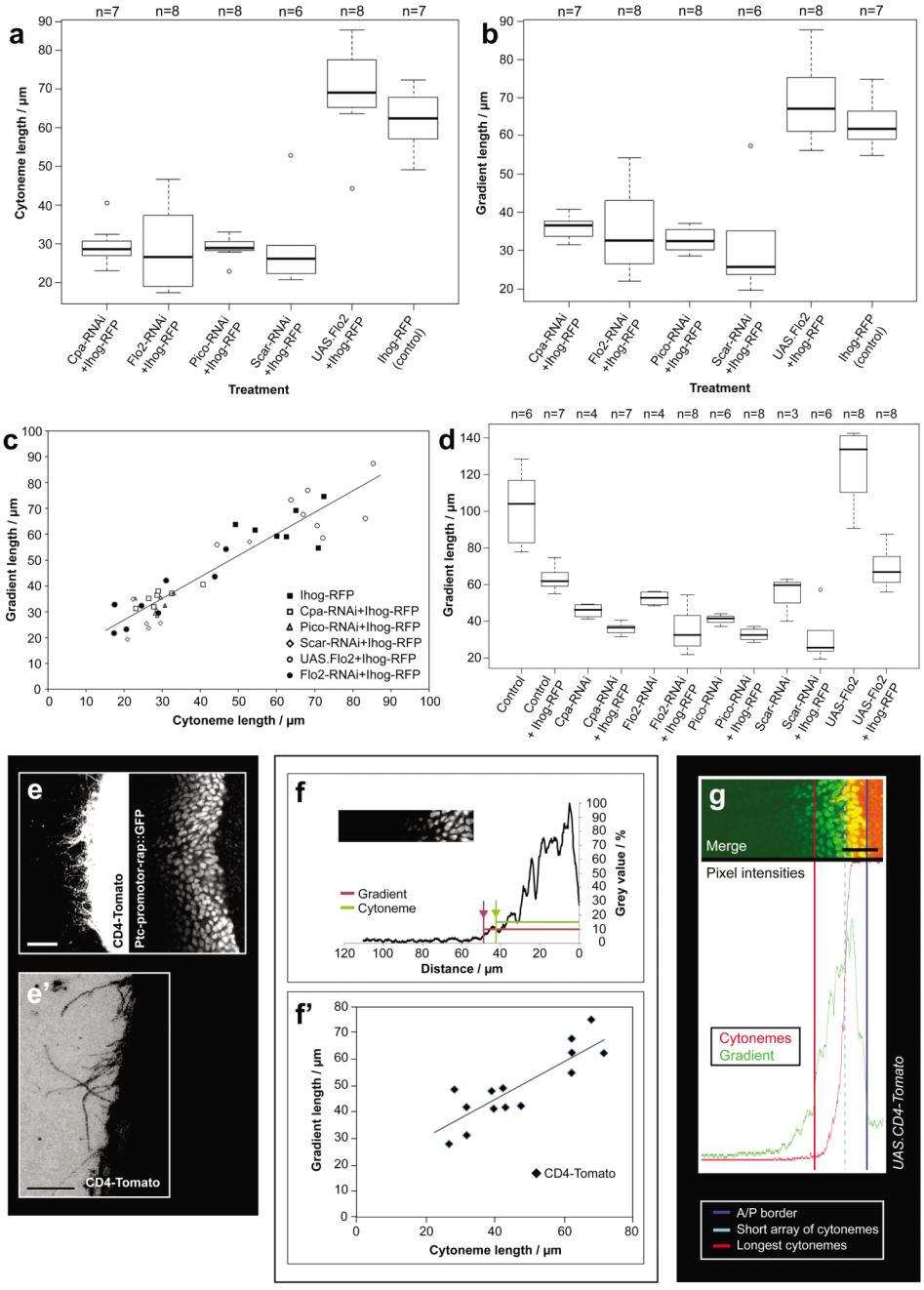

Figure 7. Gradient length correlates with cytoneme reach, both with (a-d) and without (e-g) Ihog-RFP overexpression.

(**a-c**) Experiments with Ihog-RFP overexpression. (**a**) Boxplot comparing cytoneme length between control discs and treatments affecting cytoneme formation. Boxes show median and interquartile range. Whiskers show minima/maxima, or 1.5 times interquartile range if outliers are present. Four RNAi treatments reduced cytoneme length significantly compared to *UAS.Ihog-RFP* (Kruskal-Wallis-Test, $P<0.001$ and pairwise Wilcoxon Rank Sum Test, $P<0.01$). Overexpression of Flo2 increased cytoneme length in some individuals, but with no overall significant difference from *UAS.Ihog-RFP*. (**b**) Boxplot comparing gradient length between control discs and treatments. Similar to cytoneme length, there were significant

differences between *UAS.Ihog-RFP* and four RNAi treatments (Kruskal-Wallis-Test, $P<0.001$ and pairwise Wilcoxon Rank Sum Test, $P<0.01$). Longest gradients were obtained in Flo2 overexpression. (**c**) Scatter plot of gradient length against cytoneme length, showing strong correlation (Spearman's rho= 0.89, n=44 wing discs; $P<0.001$). (**d**) Boxplot showing gradient length in control discs, *RNAi* treatments and *UAS.Flo2* treatment when co-expressed with *UAS.Ihog-RFP* or expressed alone. Expression of *UAS.Ihog-RFP* shortens the gradient (Wilcoxon Rank Sum Test; $P<0.001$). Similar to Ihog overexpression experiments (b), there are significant differences between wild-type and treatments without Ihog overexpression (Kruskal-Wallis-Test; $P<0.001$ and Wilcoxon Rank Sum Test; $P<0.05$). Fig. 6 and Supplementary Fig. S5a-f show original data. (**e-g**) Cytoneme length and Hh activity gradient length also correlate without Ihog overexpression. *hh.Gal4>UAS.CD4-Tomato* labels cytonemes and Ptc-promotor-trap::GFP visualises Hh activity gradient. Cytonemes in wing disc (**e**) and abdomen (**e'**) shown. (**f**) Quantification of gradient length and cytoneme reach in wing discs using profile plots. Graph depicts vertically averaged pixel intensities of Ptc-promotor-trap::GFP image shown in the top left corner. Red arrow indicates gradient length, up to the point where average pixel intensity drops below 5% of maximum intensity. Green arrow shows average length of the two longest cytonemes in the disc analysed. (**f'**) Scatter plot showing correlation between gradient length and cytoneme length (Spearman's rho= 0.78, n=14 wing discs; $p<0.01$). (**g**) As for Ihog-RFP overexpression (Fig. 5d; Supplementary Fig. S2), the shape of the Hh activity gradient (green profile plot) and density of cytonemes along the a-p axis (red profile plot) correlate: the short array (cyan line) coincides with the brightest gradient section, both curves decline similarly. Methods show details of statistical analysis (a-d,f). Bars, 20 μm.

Europe PMC Funders Author Manuscripts

Europe PMC Funders Author Manuscripts

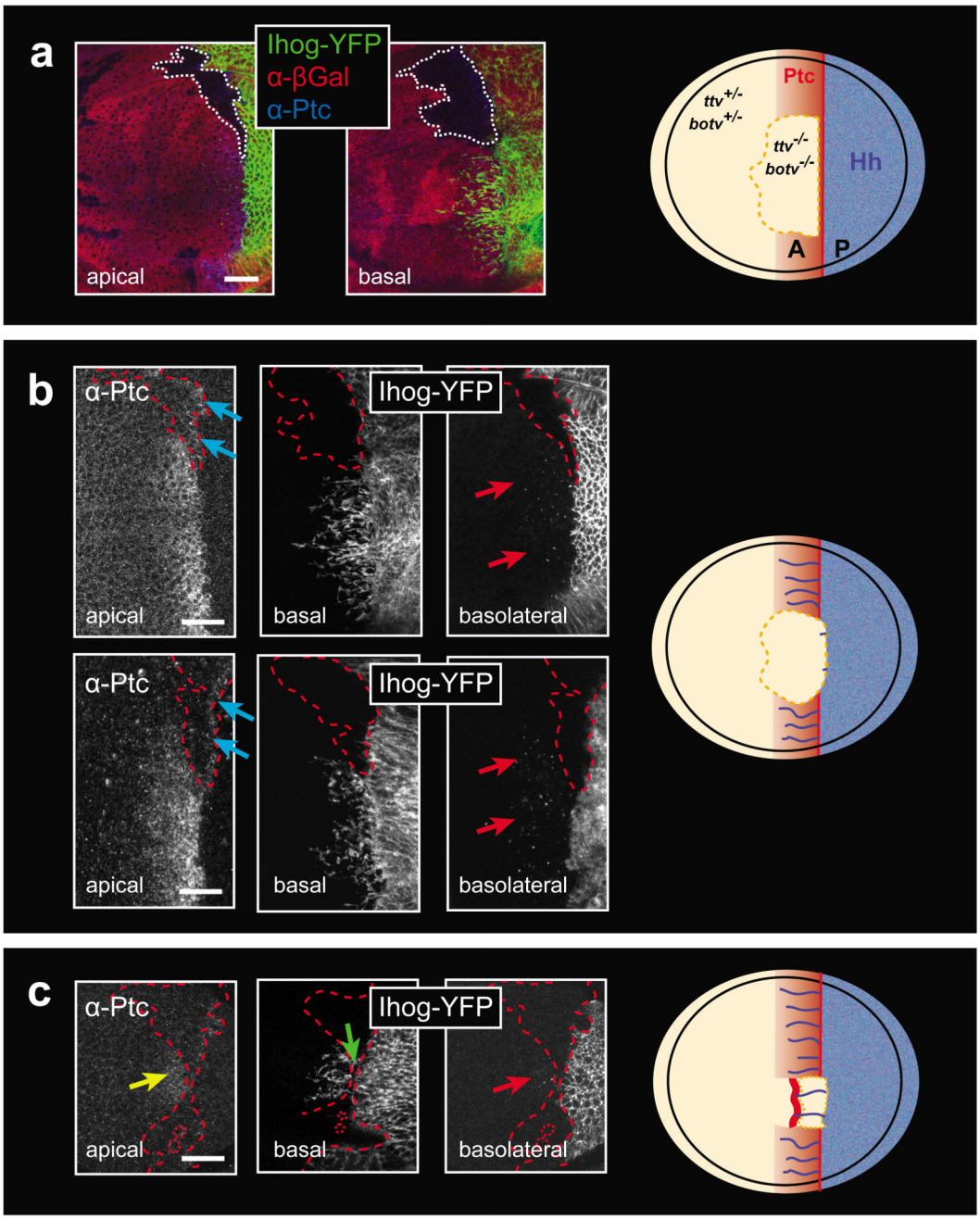

Figure 8. Cytonemes rarely cross large HSPG mutant clones, however, they do cross narrow clones.

(**a-c**) *ttv*$^{-/-}$, *botv*$^{-/-}$ double-mutant clones located at the A/P compartment border in a *Hh.Gal4>UAS.Ihog-YFP* wing disc are shown. Clones are outlined with a hatched line. (**a**) Merge of Ihog-YFP, α-Ptc and α-βGal, the absence of which labels mutant cells. Note that the clone has a very different shape in the apical and basal part of the disc. Ptc expression can be best observed in the sub-apical part and cytonemes in the basal part of the disc. A scheme shows the genotypes of the clonal and the surrounding cells as well as the areas of Hh and Ptc expression. (**b**) Two wing discs, in which cytonemes do not cross the clones. Note that the Hh signal, as assayed by Ptc expression, is not received anterior to the clones.

Only a single row of Ptc expression within the clones can be detected, as described before[52] (cyan arrows). In the heterozygous territory, however, cytonemes and Ptc expression can be observed. Note that basolaterally, Ihog puncta can be observed only in regions, in which also cytonemes are present (red arrows). (**c**) Wing disc, in which cytonemes cross a narrow area of the clones (green arrow). Note that the Hh signal, as assayed by Ptc expression, is received anterior to the clones (yellow arrows). As in (b), basolateral Ihog puncta can only be observed in regions, in which also cytonemes are present (red arrows). Bars, 20 μm.